Water quality at Chaco Culture National Historical Park and the potential effects of hydrocarbon extraction

Benjamin S. Linhoff [a],[*], Kimberly R. Beisner [a], Andrew G. Hunt [b], Zachary M. Shephard [a]

[a] US Geological Survey, New Mexico Water Science Center, USA
[b] US Geological Survey, Noble Gas Laboratory, USA

ARTICLE INFO

ABSTRACT

Study region: Chaco Culture National Historical Park (CCNHP) is in the San Juan Basin of northwestern New Mexico, U.S.A. Its only water supply is in Gallup Sandstone aquifer, stratigraphically surrounded by layers long targeted for oil and natural gas extraction.

Study focus: To assess groundwater flow direction, age, mixing between aquifers, and whether hydrocarbons extraction may affect water quality, we completed a geochemical groundwater sampling campaign. Groundwater at 11 sites was analyzed for major ions, hydrocarbon associated volatile organic carbon (VOC) compounds, noble gases, and the isotope systems δ^2H, δ^{18}O, ^{87}Sr/^{86}Sr, δ^{13}C, and ^{14}C.

New hydrological insights for the region: Results demonstrate that all sampled groundwaters are exceedingly old and geochemically evolved, with a median ^{14}C age of ~41,000 years before present and a north flowing path. Three lines of evidence suggest mixing between aquifers through relatively impermeable shale units and mixing with hydrocarbons: 1) noble gases are fractionated likely through mixing with connate water expelled during hydrocarbon genesis; 2) several wells—including the park's main supply well—contained trace amounts of hydrocarbon related VOC compounds; and 3) major ion analysis shows mixing trends between aquifers. We hypothesize that cross-aquifer mixing may be facilitated through the region's numerous hydrocarbon related boreholes. Whether our findings are the result of oil and gas extraction or represent the natural state of the aquifers will require more research.

1. Introduction

The potential effects of oil and natural gas extraction in the San Juan Basin of northwestern New Mexico, U.S.A. (Engler et al., 2015; Kelley et al., 2014; Fig. 1) on Chaco Culture National Historical Park (CCNHP) have garnered national attention (e.g. Moe, 2017 and Bryan, 2023), concern from the National Park Service (NPS), and Native American tribes. Nearly 60,000 visitors a year travel to the park, many of whom stay at the park campground. Following decades of unsuccessful attempts to develop usable near-surface water sources (C. Filippone, National Park Service, written communication, 2018), a 944-m deep well (Chaco Well, Site 602; Table 1 and Fig. 1) was constructed in the Gallup Sandstone aquifer in 1972. This provided the park with the first reliable drinking water source since it was established in 1907. All park visitors and some members from the surrounding community rely on this water source in the
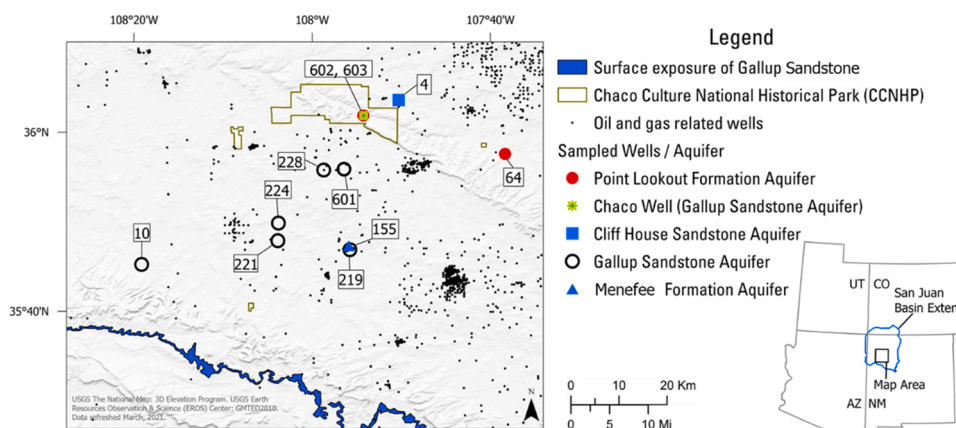
Gallup Sandstone aquifer.

Advances in unconventional hydrocarbon extraction techniques including hydrofracking (HF) have increased the potential for hydrocarbon extraction within the San Juan Basin and many other locations in the U.S.A. (U.S. Energy Information Administration, 2015). Furthermore, in the last decade, a rapid increase in hydrocarbon extraction in the San Juan Basin near CCNHP has targeted the Gallup Sandstone, Mancos Shale, and the surrounding units (Figs. 1 and 2; Engler et al., 2015; Kelley et al., 2014).

The 30–60 m thick Gallup Sandstone (Stone et al., 1983) is stratigraphically between thick confining sequences of the lower-permeability Mancos Shale (Fig. 2). Both the Mancos Shale and the Gallup Sandstone are in the San Juan Basin and both may contain oil or natural gas (Kelley et al., 2014). Available oil and gas well data—available through the State of New Mexico Oil Conservation Division (https://www.emnrd.nm.gov/ocd/#gsc.tab=0)—show that hydrocarbon wells near the park were drilled in the 1950 s through 1970 s and targeted the Dakota Formation, Entrada Sandstone, Gallup Sandstone, Mancos Shale, and Morrison Formation (Figs. 2 and 3). This scenario, whereby the drinking water aquifer is at the same depth as targeted hydrocarbons is likely unique; in general, drinking water aquifers are shallow near-surface aquifers while hydrocarbon bearing units are hundreds or thousands of meters below land surface (Meng and Ashby, 2014). Hence, the Chaco Well may be more vulnerable to contamination from hydrocarbon extraction activities than many other locations.

During HF, hydraulic fracturing fluid (HFF) is injected into a low-permeability petroleum reservoir (such as shale) under high pressure. This fractures the rock formation horizontally and vertically, increasing permeability by orders of magnitude and mobilizing fluids, such as natural gas and oil, which are induced to flow to a well where they are extracted. HF at a single site can be economically viable for decades, and a single well can undergo HF multiple times over its life cycle (Clark et al., 2013). The process is extremely water intensive, routinely requiring 4–16 million gallons of water per well (Clark et al., 2013). Following HF, between 5% and 300% of the initial HFF volume returns to the surface as flowback water (also called produced water). This produced water may be reinjected for HF or disposed of through deep well injection, wastewater treatment facilities, storage in ponds, or released onto the ground surface or into surface waters (Clark et al., 2013; Gallegos and Varela, 2015).

HFF is a mixture of water, proppants used to maintain fractures, and additives to enhance production such as lubricants, scale reducers, viscosity builders, and biocides to minimize biofouling and souring of the hydrocarbon (Mumford et al., 2018; Stringfellow et al., 2014). Self-reported chemical disclosures of fracturing fluid can be found within the FracFocus database (https://fracfocus. org/). Produced water generally has exceedingly high total dissolved solids (TDS; 1000–90,000 mg/L) with elevated Na^+, CH_4, Ba^{2+}, Br^-, B, hydrocarbons, and Ra activity (Cozzarelli et al., 2017; Cozzarelli et al., 2021; Gordalla et al., 2013; McIntosh and Ferguson, 2019; Tasker et al., 2020; Wen et al., 2021; Ziemkiewicz, Thomas, 2015). However, the composition of produced waters varies between brines and formations and is controlled by many factors. Ideally, when assessing whether groundwater is mixed with produced waters the composition of both end members is known. An additional concern is the existence of fast-flow pathways between geologic units created by the presence of uncased boreholes distributed around the San Juan Basin, many of which were used for oil and gas exploration (Lacombe et al., 1995). These boreholes as well as improperly cased or plugged boreholes have the potential to transmit fluids and gases from geologic units with high hydrostatic pressure to units with lower hydrostatic pressure (Perra, 2021). The rate at which this short-circuiting flow occurs depends on the hydrostatic pressure differences and the transmissivities of the geologic units or short circuit pathway. Short circuit fluid flow is potentially an important source of fluid migration in the region as there are many inactive oil and gas wells in the San Juan Basin (Figs. 1 and 3).

The potential for contamination from hydrocarbon extraction activities to CCNHP is largely unknown due to the lack of knowledge of groundwater flow direction, geochemical evolution, flow velocity, and mixing between aquifers. Additionally, baseline water chemistry in relevant aquifers has not been defined and contamination from HFF and produced waters has not been assessed. The objectives of this work were to complete a geochemical sampling campaign at wells within and outside of CCNHP to determine

Fig. 1. This map of the field area in the San Juan Basin in northwestern New Mexico shows the locations of sampled wells, their respective aquifers, surface exposure of the Gallup Sandstone, and the boundaries of Chaco Culture National Historical Park. Also shown are the locations of oil and gas related wells, most of which are inactive (oil and gas well locations and information is available through the State of New Mexico Oil Conservation Division: https://www.emnrd.nm.gov/ocd/#gsc.tab=0).

baseline water chemistry, assess mixing between aquifers, determine groundwater flow directions, and to evaluate whether groundwater has been contaminated or could become contaminated from nearby hydrocarbon extraction activities. Geochemical constituents measured include major ions, noble gases, and isotope systems including strontium ($^{87}Sr/^{86}Sr$), deuterium (δ^2H) and oxygen ($\delta^{18}O$) in water, and the dissolved inorganic carbon isotopes $\delta^{13}C$ and ^{14}C. We also measured volatile organic carbon (VOC) compounds including benzene, toluene, ethylbenzene, and xylene (BTEX) compounds, which are often associated with hydrocarbons.

2. Methods

2.1. Study area

Between 850 and 1250 A.D., CCNHP (Fig. 1) was the center of a sophisticated social, political, and architectural civilization with a 130,000 km^2 sphere of influence (NPS, 2015). Situated in a remote and arid region of northwestern New Mexico, CCNHP protects over 4000 sites—representing 10,000 years of continuous use (NPS, 2015)—including dozens of major complexes, monumental masonry, and earthen structures; many of these structures were the largest buildings in North America until the late 19th century (Lekson, 1984). CCNHP is a United Nations Educational, Scientific and Cultural Organization (UNESCO) World Heritage Site as well as an important religious site for Native Americans (https://whc.unesco.org/en/list/353/).

While this study focused on sampling wells screened within the Gallup Sandstone, wells were also sampled in the Point Lookout Sandstone, Menefee Formation and Cliff House Sandstone (Fig. 2). The Gallup Sandstone is surrounded by the Mancos Shale and consists of sandstone, shale, and coal. The Chaco Well is located near the Gallup Sandstone's northern extent (Fig. 1). The Point Lookout Sandstone is stratigraphically above the Mancos Shale and is composed largely of sandstone. The Menefee Formation, in contrast, is composed of interbedded shale, sandstone, and coal (Kelley et al., 2014). Stratigraphically above this, the Cliff House Sandstone is largely composed of sandstone. All units described above are known to contain oil or natural gas within the San Juan Basin (Brister and Hoffman, 2002).

Previous studies in the San Juan Basin found that groundwater in the Morrison Formation (stratigraphically below the Mancos Shale; Fig. 2) had too little ^{14}C to effectively date, concluding that groundwater likely recharged > 52,000 years before present (ybp; Dam, 1995). Past research has found that recharge to the Gallup Sandstone generally occurs where the unit crops out at the surface ~ 55 km to the south of the Chaco Well (Fig. 1; Stone et al., 1983) and that groundwater generally flows from the south to the north through the Gallup Sandstone (Kernodle, 1996). However, more recent groundwater withdrawals and hydrocarbon extraction across the San Juan Basin may have altered groundwater flow paths.
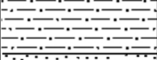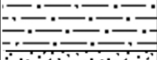
2.2. Field sample collection

Groundwater samples were collected for water chemistry analyses from 11 wells in 2019 and 2020 following U.S. Geological Survey protocols (U.S. Geological Survey, 2021). Sites were sampled once except for wells 602 and 603, which were sampled three times for VOCs. Where possible, historical data (pre-2019) is also presented from the U.S. Geological Survey National Water Information System (NWIS; U.S. Geological Survey, 2021). Wells sampled were artesian—discharging at the surface—except for Sites 4 and 10, which were subartesian and sampled via windmill pump. pH, temperature, water temperature, specific conductance (SC), and dissolved oxygen (O$_2$) were measured in a flow-through cell prior to sampling at each site (Table 2). Total dissolved solids (TDS) were estimated as the sum of dissolved major ion constituents. Groundwater was discharging at the surface at all sites prior to sampling (either through windmill pump or artesian flow), hence, no purge volume was recorded. Sample bottles were filled following field parameter stabilization. Water samples were filtered through a GWV capsule 0.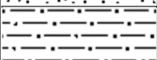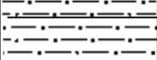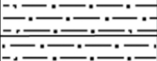45 μm filter for major cations, trace elements, alkalinity, nutrients, and carbon and strontium isotopes. Samples collected for VOCs, tritium (^3H), and stable isotopes were unfiltered. Major cations, trace elements, and strontium isotope samples were preserved to pH < 2 by adding ultrapure nitric acid. VOC samples were collected in triplicate 40-mL septum capped amber glass vials, filled from the bottom using a high density polyethylene tube until

Table 1
This table shows the project Site Identification Number (ID) and the USGS Site number as well as location and information about the well and groundwater elevation. A * symbol is used for well depth elevation (el.) where only the hole depth was available. Abbreviations Ss and Fm stand for sandstone and formation respectively. Data from U.S. Geological Survey (2021).

Site ID	USGS Site ID	Aquifer	Lattitude	Longitude	Sample Date	Water Level	Site	Groundwater	Well Depth
						(m)	el. (m)	el. (m)	(m)
4	360336107501801	Cliffhouse	36.06000	-107.83834	8/28/2019	23.38	1931	1907.23	153.92
10	354514108190601	Gallup	35.75391	-108.31896	8/27/2019	48.77	2055	2006.50	393.80
219	354653107554401	Gallup	35.78141	-107.92951	5/31/2019	-8.12	1996	2004.56	350.52
221	354753108034901	Gallup	35.79807	-108.06423	5/30/2019	-16.64	1962	1978.94	504.44
224	354951108034501	Gallup	35.83085	-108.06312	5/30/2019	-20.47	1935	1955.95	1011.94 *
228	355547107584001	Gallup	35.92974	-107.97840	5/29/2019	-24.64	1945	1969.27	887.58
601	355553107562301	Gallup	35.93141	-107.94034	5/29/2019		1951	1951.02	998.22 *
602	360152107541401	Gallup (Chaco Well)	36.03111	-107.90383	8/3/2017	-55.47	1895	1950.42	941.83
155	354724107555201	Menefee fm.	35.79002	-107.93173	5/30/2019		1999	1999.49	
64	355735107382101	Point Lookout	35.95984	-107.63914	8/29/2019		1997	1997.05	511.45
603	360152107541301	Point Lookout	36.03113	-107.90423	1/29/2020	-30.11	1891	1921.40	570.59

Fig. 2. Stratigraphy of major geological units in the San Juan Basin. Samples for this study were collected in the Gallup Sandstone, Point Lookout Sandstone, Cliff House Sandstone, and Menefee Formation.
Geologic symbols adapted from Federal Geographic Data Committee (2006).
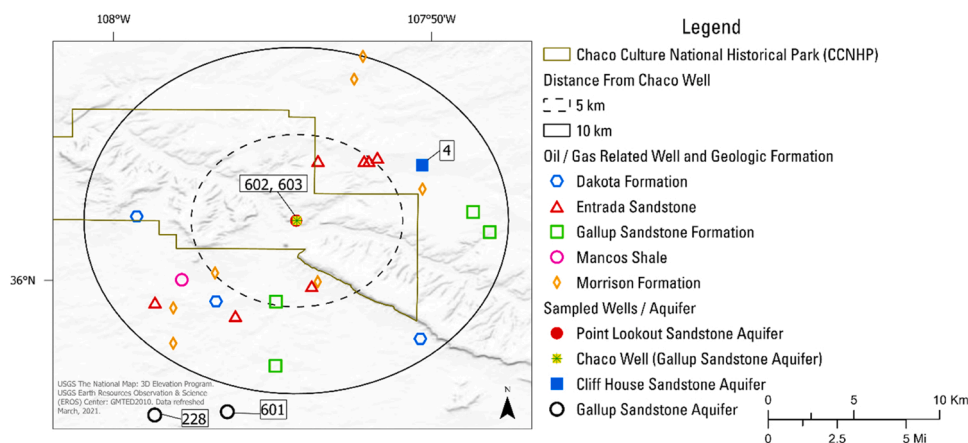
Fig. 3. All known hydrocarbon related boreholes within a 10 km radius of the Chaco Well (602). Oil and gas well locations and information is available through the State of New Mexico Oil Conservation Division: https://www.emnrd.nm.gov/ocd/#gsc.tab= 0.

no air bubbles or headspace remained and then acidified to pH< 2 with 1:1 HCl:H$_2$O. Similarly, carbon isotope samples were collected in 1-L glass bottles filled from the bottom and allowed to flush three bottle volumes before being capped with a polycone cap with no headspace. Tritium samples were collected in 1-L poly bottles following the same bottom filling procedure and cone cap as the carbon isotope samples. Noble gas samples were collected in copper tubes in duplicate; back pressure was applied with a restrictor on the sample tubing past the copper tube to minimize bubble formation prior to sealing the samples with refrigerator clamps (Weiss, 1968). Field alkalinity was computed from titration data using the incremental equivalence method (USGS, 2021). All samples were kept below 4°C following sample collection. Water levels at windmill sites were measured after stopping the windmill for several hours until groundwater levels were stable. At artesian sites, water levels were measured using a pressure transducer.

Table 2

Field parameters and nutrient concentrations used for this study. While this study collected samples in 2019 and 2020, historical sampling results from the USGS National Water Information System database are also provided for comparison. Data from U.S. Geological Survey (2021).

Site ID	Date	Temperature	SC	TDS	Alkalinity	O2	pH (field)	NH3 +NH4	NO2-	NO3-	NO3 +NO2	PO4
		°C	μS/cm	mg/L	mg/L (as CaCO3)	mmol/L	field	mmol/L as N	mmol/L as N	mmol/L as N	mmol/L as N	mmol/L as PO4
Median		21.2	2800	1940	302	0.009	8.5	0.055				
Mean		22.6	3151	2084	434	0.011	8.5	0.050				
4	28–03–1978	14	3000	2350			8.3				0.004	0.0003
4	28–08–2019	18.6	2930	2270	473	0.009	7.8	0.051	< 0.0001	< 0.003	< 0.003	0.0003
10	27–08–2019	21.8	1400	900	176	0.022	8.1	0.024	0.001	< 0.003	< 0.003	0.0002
219	31–05–2019	20.6	3970	2960	362	0.025	8.5	0.056	< 0.0001	< 0.003	< 0.003	0.0003
221	30–05–2019	15	1230	871	264	0.025	9	0.021	< 0.0001	< 0.003	< 0.003	0.0004
224	30–05–2019	14.2	1250	795	265	0.001	9.2	0.022	< 0.0001	< 0.003	< 0.003	0.0006
228	29–05–2019	28.1	2420	1940	225	0.006	8.6	0.057	< 0.0001	< 0.003	< 0.003	0.0003
601	21–04–1986	32.7	2900	1910			8.6					
601	29–05–2019	33.5	2920	1990	210		8.6	0.053	< 0.0001	< 0.003	< 0.003	0.0003
601	27–08–2019	33.3	2680			0.013	8.5					
602	22–04–1986	32.8	2720	1810			8.2					
602	21–10–1987	32.9	2800	2030	290		8.3	0.033	< 0.0001	< 0.003	< 0.003	0.0006
602	22–08–2017	20.5	2800	1860	302	0.003	8.7	0.059	< 0.0001	0.003	0.003	0.0003
602	28–05–2019	15.4	2800	1920	313	0.013	8.3	0.056	< 0.0001	< 0.003	< 0.003	0.0002
155	30–05–2019	15	5710	3910	379	0.003	8.5	0.075	< 0.0001	< 0.003	< 0.003	0.0002
64	29–08–2019	21.7	1750	1150	734	0.009	8.7	0.024	< 0.0001	< 0.003	< 0.003	0.0010
603	10–11–1987		5500	3270			8.1	0.086	< 0.0001	< 0.003	< 0.003	0.0003
603	29–05–2019	14.5	5280	3500	1650	0.001	8.6	0.088	< 0.0001	< 0.003	< 0.003	0.0008
603	04–06–2020	21.7	5800			0.013	8.4					

2.3. Water chemistry analytical methods

Water samples were analyzed for major cations, trace elements, and nutrients by the USGS National Water Quality Laboratory (NWQL) in Denver, Colorado. Inductively coupled plasma atomic emission spectrometry was used to analyze for cations including calcium (Ca^{2+}), total iron (Fe), magnesium (Mg^{2+}), manganese (Mn^{2+}), potassium (K^+), and sodium (Na^+) (Fishman, 1993). Chloride (Cl^-), fluoride (F^-), and sulfate (SO_4^{2-}) were analyzed by ion chromatography, and dissolved silica (SiO_2) was analyzed by discrete analyzer colorimetry (Fishman and Friedman, 1989). Nitrate (NO_3) plus nitrite (NO_2) was analyzed by colorimetry (Patton and Kryskalla, 2011). Twenty-three VOC compounds were analyzed by gas chromatography/mass spectrometry (Rose et al., 2016; Connor et al., 1998). Quality assurance and quality control (QA/QC) samples include three field blank samples using certified inorganic blank water, two field blank samples with nitrogen purged organic blank water for VOC analysis, two replicate samples, and three laboratory spikes for VOC samples. Results and discussion of the QA/QC samples are presented in Supplemental Material.

Stable isotope ratios ($\delta^{18}O$ and δ^2H in H_2O) were measured at the USGS Reston Stable Isotope Laboratory in Reston, Virginia. Samples were analyzed using mass spectrometry following methods by Révész and Coplen (2008). Two-sigma uncertainties are 0.2‰ for $\delta^{18}O$ and 2‰ for δ^2H reported relative to Vienna Standard Mean Ocean Water (VSMOW). Strontium (Sr) isotope ratios ($^{87}Sr/^{86}Sr$) were measured by the USGS National Research Program Laboratory in Menlo Park, California by using multi-collector mass spectrometry following methods described in Bullen et al. (1996); results were precise to 0.00002 or better at the 95-percent confidence level. Noble gases helium (He), neon (Ne), argon (Ar), krypton (Kr), and xenon (Xe) were analyzed by the USGS Noble Gas Laboratory in Lakewood, Colorado using methods described in Hunt (2015). The University of Miami Tritium Laboratory in Miami, Florida measured tritium in samples using electrolytic enrichment and gas counting, with a reporting limit of 0.3 pCi/L. Mineral saturation indexes (SI) were calculated using Geochemist's Workbench (version 15.0; Aqueous Solutions, LLC, Champaign, Illinois).

2.4. Dating groundwater using carbon isotopes

Carbon isotopes—percent modern carbon-14 (PMC) and $\delta^{13}C$—were analyzed by the National Ocean Sciences Accelerator Mass Spectrometry (NOSAMS) at the Woods Hole Oceanographic Institution, Massachusetts using accelerator mass spectrometry. To estimate the initial ^{14}C present in these samples ($^{14}C_\circ$), we used the program NETPATHXL (Parkhurst and Charlton, 2008; Han and Plummer, 2016) which calculates $^{14}C_\circ$ using the Fontes and Garnier model (Han and Plummer, 2013). This model corrects for the effect of carbon exchange between dissolved inorganic carbon (DIC) and solid carbonate and soil, the major unknowns are the isotopic composition of solid carbonates and soil gas.

Once $^{14}C_\circ$ was estimated, age was determined through Eq. (1).

$$t = -\frac{5730}{ln2} ln\left(\frac{^{14}C_{DIC}}{^{14}C}\right) \tag{1}$$

where t is the groundwater age in years, 5730 is the half-life of $^{14}C_\circ$, $^{14}C_{DIC}$ is the PMC measured in the sample and $^{14}C_\circ$ was the initial ^{14}C present calculated through NETPATHXL assuming solid carbonate exchange is the dominant process impacting the carbon isotopes.

2.5. Noble gas solubility modeling

Noble gas composition is initially set during recharge to an aquifer and is controlled by the partial pressure of the gas phase (mole fraction multiplied by atmospheric pressure), temperature, salinity, and the amount of excess gas entrapped during recharge (e.g. Heaton and Vogel, 1981). An estimate of the initial temperature of water during recharge can be determined by the application of a solubility-based model which takes the measured noble gas compositions and fits the modeled recharge parameters to the data (Aeschbach-Hertig et al., 1999).

We utilized the closed equilibrium (CE) model developed by Aeschbach-Hertig et al. (1999) for noble gas solubility modeling and the DGMETA (Dissolved Gas Modeling and Environmental Tracer Analysis; Jurgens et al., 2020) model to resolve noble gas recharge parameters. Work by Stute and Sonntag (1992), Aeschbach-Hertig et al. (1999), Heaton and Vogle (1981), and Ballentine et al. (2002) showed that excess air components trapped during recharge can vary in composition depending on the degree of equilibration of the trapped air, gas losses, and fractionation of the original air-like component. For implementation of the CE model, measured dissolved noble gas components are compared to modeled concentration values using estimated parameters of temperature (T), initial concentration of entrapped air (Ae), and the reduction of entrapped volume by dissolution and compression, with the assumption that the water was fresh (or low salinity) and the partial pressure of the gases is associated with atmospheric pressure at the elevation of the water table (~1994 m). An error-weighted least squares fit was used to solve for free model parameters (T and Ae) by minimizing chi squared.

All data that support the results and conclusions in this study are available from U.S. Geological Survey (2021) by using the USGS Site Number in Table 1 to compile the data.

3. Results

3.1. Groundwater chemistry and elevation results

In the Gallup Sandstone aquifer, groundwater elevation was highest in the south and lowest in the north implying south to north groundwater flow (Table 1); this is consistent with the findings of Kernodle (1996). SC and TDS were highest in the Menefee Formation aquifer (Well 155; 5710 μS/cm and 3910 mg/L, respectively) and the Point Lookout Sandstone aquifer at Well 603 (Table 2). Generally, sampled wells had low O_2 concentrations (0.003–0.025 mmol/L O_2), basic pH (7.8–9.2) and low nitrogen and phosphorous (Table 2).

3.2. Noble gas and isotopic results

Noble gas concentrations—shown in Table 3—varied across the field site with Wells 228 and the Chaco Well (Gallup Sandstone aquifer) generally having the highest noble gas concentrations and Well 603 (Point Lookout Sandstone aquifer) having the lowest (with the exception of ^{4}He). For the seven sites sampled for noble gases, median Ne, ^{4}He, Ar, Kr, and Xe values were 3.49×10^{-7}, 6.99×10^{-6}, 4.53×10^{-4}, 9.4×10^{-8}, and 9.6×10^{-9} cm^3/g, respectively (Table 3).

The stable isotopes of water (δ^2H and δ^{18}O) were heaviest at Well 64 (Point Lookout Sandstone aquifer) and lightest at Well 228 (Gallup Sandstone aquifer). In the Gallup Sandstone aquifer, δ^2H and δ^{18}O isotopes were light with respect to other aquifers except for Well 219 which was heavier than the other Gallup Sandstone aquifer samples (Fig. 4). Well 602 (Chaco Well) had higher ^{87}Sr/^{86}Sr values (0.70922) then the rest of the data set (Table 4).

3.3. Groundwater age—tritium and carbon isotopes

Tritium concentrations at all sites were below the instrument detection limit (^{3}H <0.3 pCi/L; Table 4). Carbon-14 results were very low (<1 PMC) except for Well 10 (3.59 PMC; Table 4) in the Gallup Sandstone aquifer in the southern portion of the field area. δ^{13}C values ranged from $-17.5‰$ to $-7.55‰$ across the study area with the highest values at Well 155 ($-7.55‰$) and the lowest at Well 4 ($-17.5‰$).

The lack of detectable tritium in groundwaters likely indicates no mixing with modern waters (Table 4; Linhoff, 2022; Lindsey et al., 2019; Travis et al., 2021). In the absence of inputs from modern waters, carbon isotopes are generally useful indicators of geochemical processes and may help constrain groundwater age. Dam (1995) measured carbon isotopes in the San Juan Basin as part of a larger groundwater chemistry study; in that study, ^{14}C varied between < 0.4 PMC to 6.4 PMC and δ^{13}C varied from -7.6 to $-26.1‰$ in seven samples collected from the Gallup Sandstone aquifer.

When interpreting groundwater ages, chemical processes that alter the initial ^{14}C of dissolved inorganic carbon (DIC) in groundwater must be considered (Cartwright et al., 2020). A graphical method (Fig. 5) developed by Han et al. (2012) and Han and Plummer (2013, 2016) was used to recognize processes that might prevent accurate assessment of whether a sample contained ^{14}C that had undergone decay. The method uses the PMC, δ^{13}C, and HCO$_3^-$ composition of a sample to determine the suitability of a groundwater for age dating. The two triangles in Fig. 5 represents the "zero-age" zone; these were constructed according to Han and Plummer (2016) using soil gas δ^{13}C values of -20 and $-25‰$ from Dam (1995). The soil gas δ^{13}C values are based on Gallup Sandstone aquifer groundwater in the likely recharge zone south of the field site where the Gallup Sandstone crops out (Fig. 1). In Fig. 5, all samples plot below the zero-age region and hence are likely old groundwater that has undergone ^{14}C decay and may be dated.

Well 10 in the Gallup Sandstone was the youngest water (~23,000 ybp) followed by Well 4 (37,000 ybp) in the Cliff House Sandstone (Table 4 and Fig. 2). Five samples had PMC lower than the method can accurately date and hence are assumed to be older than 52,000 ybp (Table 4). Older ages were found in the northern portion of the field area implying south to north groundwater flow. These age estimates do not take into account potential redox reactions. All sites had relatively low dissolved O_2 concentrations as well as reduced forms of nitrogen ($NH_3 + NH_4$) and CH_4; this could cause an overestimate of ^{14}C ages (Han et al., 2012).

Table 3

Results of noble gas analyses including neon (Ne), helium-4 (^{4}He), argon (Ar), krypton (Kr), and xenon (Xe). Uncertainty is the published method uncertainty in Hunt (2015). Data from U.S. Geological Survey (2021).

Site ID	Date	Ne cm^3/g	±	^{4}He cm^3/g	±	Ar cm^3/g	±	Kr cm^3/g	±	Xe cm^3/g	±
Median		3.49E-07		6.99E-06		4.53E-04		9.40E-08		9.60E-09	
Mean		3.41E-07		1.37E-05		4.40E-04		8.76E-08		8.99E-09	
219	5/31/2019	2.77E-07	5.50E-09	3.94E-06	1.87E-08	4.14E-04	8.28E-06	8.90E-08	2.60E-09	9.60E-09	2.00E-10
221	5/30/2019	3.75E-07	7.50E-09	5.54E-06	2.63E-08	4.75E-04	9.51E-06	9.80E-08	2.90E-09	1.08E-08	3.00E-10
224	5/30/2019	3.71E-07	7.40E-09	4.99E-06	2.36E-08	4.81E-04	9.63E-06	9.80E-08	2.90E-09	1.14E-08	3.00E-10
228	5/29/2019	4.18E-07	8.30E-09	1.03E-05	4.90E-08	5.06E-04	1.01E-05	1.01E-07	3.00E-09	1.11E-08	3.00E-10
602	8/22/2017	3.48E-07	5.20E-09	1.95E-05	1.61E-07	4.53E-04	7.18E-06	9.40E-08	2.10E-09	9.30E-09	4.00E-10
155	5/30/2019	3.49E-07	6.90E-09	6.99E-06	3.32E-08	4.40E-04	8.80E-06	8.50E-08	2.50E-09	8.10E-09	2.00E-10
603	5/29/2019	2.48E-07	4.90E-09	4.45E-05	2.11E-07	3.11E-04	6.23E-06	4.79E-08	1.40E-09	2.60E-09	0.00E+00
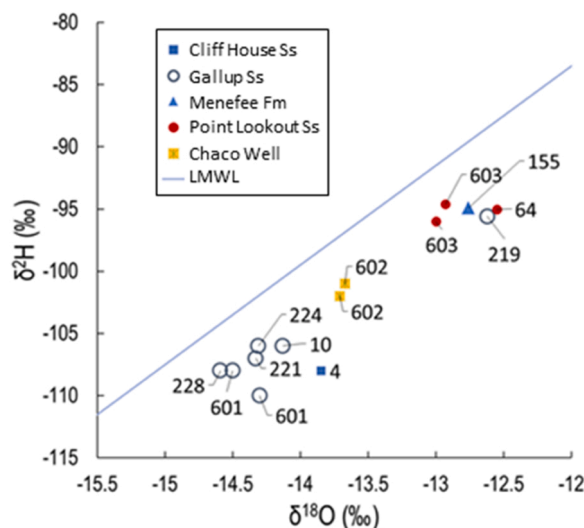
Fig. 4. Results from $\delta^{18}O$ and δ^2H analyses along with the local meteoric water line (LMWL) from (Vuataz and Goff, 1986). These data may represent a shifted meteoric water line or a past drier environment (Section 4.2). Abbreviations Ss and Fm stand for Sandstone and Formation, respectively.

Table 4

Results of isotope analyses of carbon (percent modern carbon (PMC) and $\delta^{13}C$), tritium (^3H), strontium ($^{87}Sr/^{86}Sr$), deuterium (δ^2H), and oxygen ($\delta^{18}O$). Also shown are estimated radiocarbon ages in years before present (ybp) of groundwater using soil gas $\delta^{13}C$ values of $-20‰$ and $-25‰$. Five samples had radiocarbon ages greater than the method can resolve ($>52,000$ ybp). Data from U.S. Geological Survey (2021).

| Site	Data	^{13}C	^{14}C	^{14}C	^{14}C	Age ($-20‰$ soil gas ^{13}C)	Age ($-25‰$ soil gas ^{13}C)	^3H	$^{87}Sr/^{86}Sr$	δ^2H	$\delta^{18}O$
		‰	pmc	denormalized pmc	error pmc	ybp	ybp	(pCi/L)		‰	‰
Median		-11.42	0.21	0.22		44865	42921		0.70848	-104	-13.8
Mean		-11.56	0.55	0.56					0.70858	-102	-13.7
4	28–08–2019	-17.48	0.78	0.79	0.06	38,688	36,832	< 0.3		-108	-13.85
10	27–08–2019	-14.19	3.59	3.64	0.07	24,266	22,380	< 0.3		-106	-14.13
219	31–05–2019	-7.85	0.15	0.15	0.05	> 52,000	> 52,000	< 0.3	0.70843	-95.6	-12.62
221	30–05–2019	-12.31	0.31	0.32	0.06	43,194	41,369	< 0.3	0.70844	-107	-14.33
224	30–05–2019	-12.56	0.37	0.38	0.05	41,905	40,087		0.70837	-106	-14.31
228	29–05–2019	-12.45	0.26	0.26	0.05	44,865	42,921	< 0.3	0.70862	-108	-14.59
601	21–04–1986								0.70865	-110	-14.3
601	29–05–2019									-108	-14.5
602	22–08–2017	-10.07	0.06	0.06	0.06	> 52,000	> 52,000	< 0.3		-101	-13.67
602	28–05–2019	-10.05	0.17	0.17	0.06	> 52,000	> 52,000	< 0.3	0.70922	-102	-13.71
155	30–05–2019	-7.55	0.21	0.22	0.05	42,093	40,266	< 0.3	0.70841	-94.9	-12.76
64	29–08–2019	-11.42	0.05	0.05	0.06	> 52,000	> 52,000	< 0.3		-95	-12.55
603	10–11–1987									-96	-13
603	29–05–2019	-11.23	0.1	0.1	0.05	> 52,000	> 52,000	< 0.3	0.70851	-94.6	-12.93

3.4. Major ion results

The major ion composition differs markedly between aquifers (Fig. 6, Table 5). Notably, Mg^{2+} and Ca^{2+} are relatively high in the Cliff House Sandstone and Cl^- and HCO_3^- are elevated in groundwaters in the Point Lookout Sandstone. SO_4^{2-}, Cl^-, and Na^+ are also quite different between each aquifer with the Point Lookout Sandstone and Menefee Formation waters having elevated Na^+ and Cl^-. The Gallup Sandstone—where the Chaco Well is screened—generally has relatively low Ca^{2+}, Mg^{2+}, Cl^- and HCO_3^- with elevated SO_4^{2-} concentrations. In general, all groundwater sites in the study were near calcite and quartz equilibrium and were supersaturated (mineral saturation index (SI) > 0) with dolomite and undersaturated (SI < 0) with respect to gypsum and halite (Table 6). Both calcite and gypsum are very common secondary minerals and may be found in all rock types.

3.5. Organic compound detections

VOC were detected at five sites in the study area (Table 7). All samples with VOC detections were from the Gallup Sandstone and
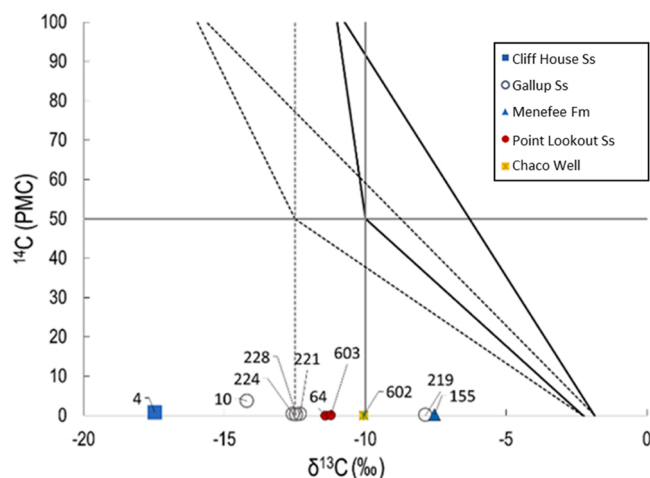
Fig. 5. Samples collected in this study have very low percent modern carbon (PMC) content and variable $\delta^{13}C$ values likely reflecting very old waters with multiple pathways of geochemical evolution. In this figure, solid black lines represent the zero-age area using –20 $\delta^{13}C$ for soil gas and the dashed lines were created using –25 $\delta^{13}C$ for soil gas. According to Han and Plummer (2013), samples that plot below the zero-age triangles likely contain old carbon that may be dated.
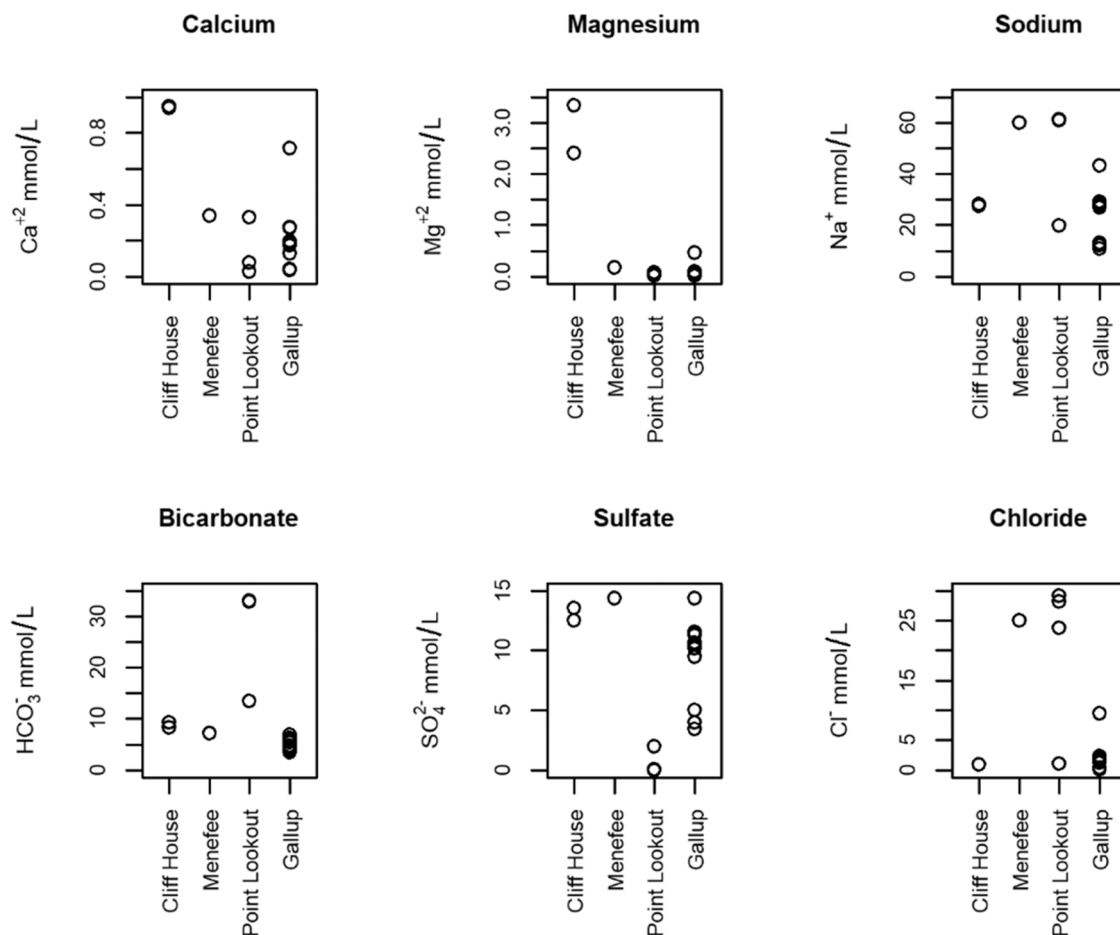
Fig. 6. Major ion concentrations in mmol/L of the four aquifers sampled. Plots represent Cliff House aquifer (n = 2), Menefee Formation aquifer (n = 1), Point Lookout Sandstone (n = 3), and the Gallup Sandstone aquifer (n = 11).

Table 5

Results of major ion and total dissolved inorganic carbon (TDIC), dinitrogen (N_2), and methane (CH_4) analyses used in this study. Data from U.S. Geological Survey (2021).

Site ID	Date	HCO3	TDIC	Ca2 +	Mg2 +	Na+	K+	Cl-	Br-	SO42-	F-	SiO2	Ba	N2	CH4
		mmol/L	mmol/L	mmol/L	mmol/L	mmol/L	mmol/L	mmol/L	mmol/L	mmol/L	mmol/L	mmol/L (as SiO2)	μmol/L	mmol/L	mmol/L
Median		6.01	31.43	0.20	0.09	27.49	0.08	1.33	0.00	10.41	0.08	0.22	0.12	0.98	0.00
Mean		9.36	48.68	0.30	0.42	31.32	0.09	6.02	0.00	8.48	0.11	0.23	9.01	0.94	0.00
4	28–03–1978	8.36	42.80	0.95	3.33	27.40	0.12	0.96		13.53	0.021	0.16			
4	28–08–2019	9.29	48.76	0.94	2.40	28.10	0.09	0.89	0.0039	12.49	0.020	0.17	0.05		
10	27–08–2019	3.46	17.97	0.71	0.46	10.92	0.07	0.15	0.00059	5.01	0.026	0.19	0.18		
219	31–05–2019	6.83	35.86	0.20	0.10	43.24	0.11	9.51	0.0072	14.37	0.134	0.18	0.06	0.83	0.0053
221	30–05–2019	4.74	25.43	0.04	0.01	13.09	0.03	0.35	0.0010	3.98	0.061	0.22	0.06	1.01	0.0039
224	30–05–2019	4.46	24.72	0.04	0.01	12.05	0.03	0.38	0.0011	3.41	0.049	0.22	0.04	1.00	0.0037
228	29–05–2019	4.24	22.26	0.13	0.03	27.49	0.07	1.81	0.0015	11.24	0.041	0.27	0.12	1.10	0.0055
601	21–04–1986	3.92	20.91	0.17	0.05	29.14	0.06	2.28	0.0025	10.41	0.037	0.28	0.73		
601	29–05–2019	3.88	20.58	0.19	0.05	28.32	0.07	2.10	0.0016	11.56	0.038	0.27	0.13		
602	22–04–1986	6.15	31.53	0.27	0.09	27.40	0.08	1.33	0.0023	9.47	0.084	0.28	0.12		
602	21–10–1987	5.47	28.85	0.18	0.10	29.14	0.08	1.38	0.00088	11.45	0.084	0.27			
602	22–08–2017	5.88	30.37	0.27	0.09	26.97	0.08	1.20	0.0020	10.14	0.076	0.28	0.12	0.97	0.0038
602	28–05–2019	6.01	31.43	0.27	0.09	27.10	0.09	1.26	0.0018	10.62	0.082	0.26	0.12	0.99	0.0032
155	30–05–2019	7.26	37.85	0.34	0.17	60.03	0.16	24.93	0.0140	14.37	0.17	0.18	0.07	0.78	0.0070
64	29–08–2019	13.37	71.38	0.03	0.01	19.83	0.03	1.05	0.0039	1.99	0.33	0.24	0.40		
603	10–11–1987	32.78	168.5	0.07	0.07	60.90	0.14	23.69	0.0044	0.048	0.18	0.22	72.82		
603	29–05–2019	32.99	168.3	0.33	0.07	61.33	0.18	29.05	0.0161	0.0026	0.46	0.20	60.15	0.83	0.0053

Table 6
Calculated mineral saturation indexes.

Site ID	Date	Dolomite	Quartz	Talc	Calcite	Gypsum	Halite
4	28–03–1978	3.21	0.19	4.19	0.85	-1.38	-6.36
4	28–08–2019	2.18	0.22	0.91	0.41	-1.39	-6.38
10	27–08–2019	1.45	0.28	1.18	0.35	-1.63	-7.49
219	31–05–2019	1.15	0.22	0.79	0.25	-2.06	-5.18
221	30–05–2019	0.64	0.26	1.85	0.06	-3.01	-7.05
224	30–05–2019	0.91	0.22	2.66	0.26	-3.04	-7.04
228	29–05–2019	0.43	0.39	0.90	0.01	-2.25	-6.07
601	21–04–1986	0.68	0.42	1.49	0.13	-2.13	-5.94
601	29–05–2019	0.67	0.39	1.32	0.15	-2.06	-5.99
602	21–10–1987	0.48	0.42	-0.05	-0.10	-2.08	-6.16
602	22–08–2017	1.68	0.40	2.82	0.59	-1.95	-6.25
602	28–05–2019	0.92	0.39	0.40	0.21	-1.93	-6.23
155	30–05–2019	1.64	0.22	1.55	0.48	-1.89	-4.63
64	29–08–2019	0.53	0.34	-0.46	0.07	-3.49	-6.41
603	10–11–1987	1.35	0.33	-1.21	0.18	-4.90	-4.63
603	29–05–2019	2.80	0.26	1.21	1.24	-5.61	-4.54

Point Lookout Sandstone. Four out of five of those sites had detections of multiple VOCs. This includes BTEX compounds, which are known to be associated with hydrocarbon deposits, flowback water, and many adverse health effects (Njobuenwu et al., 2005; Ziemkiewicz, Thomas, 2015; McMahon et al., 2017; Spycher et al., 2017; Ran et al., 2018; Karolyte et al., 2021). Eleven organic compounds were detected in samples from this study (Table 7). Organic compound detections were at low concentrations but were greater than the laboratory detection level. Benzene was the most frequently detected organic compound found at five sites (64, 228, 601, 602, and 603). Wells 64 and 603 had the greatest number of organic compounds detected, and these two wells are both from the Point Lookout Sandstone. Concentrations at Well 64 were generally higher than at Well 603, but both had low level concentrations. Well 602 was sampled by USGS in 2017 during a regional sampling effort for wells in the Colorado Plateaus physiographic province which included other organic compounds. Butane (0.398 μg/L) and hexane (0.073 μg/L) were detected in the 2017 sample above the laboratory detection level.

4. Discussion

4.1. Noble Gases

Dissolved noble gases are often useful in deciphering groundwater recharge sources and temperature, as well as assessing past mixing with hydrocarbons and groundwater age (Aeschbach-Hertig et al., 1999; Ballentine et al., 2002; Byrne et al., 2020; Heaton and Vogle 1981; Solder et al., 2020; Stute and Sonntag, 1992). Noble gas concentrations (Table 3) could not be fitted to the CE model using DGMETA (Jurgens et al., 2020) based on probable elevation and mean annual temperature parameters for the area. This inability to fit using likely recharge parameters assumes groundwater followed simple recharge into the aquifer and that no further noble gas partitioning occurred post isolation from the atmosphere. Hence, estimating the recharge temperature of groundwater across the field area using noble gases is not possible.

In groundwater, the heavier noble gases (Kr and Xe) are typically enriched relative to the light gases (He and Ne), however in this study, in all sampled sites the light noble gases were enriched relative to the heavier noble gases. No samples plot close to estimated air saturated water (ASW) or trend with air addition (excess air) from ASW (as the CE model would predict) (Fig. 7). Instead, the lower FXe values indicate a depletion in Xe concentrations relative to ^{36}Ar, and the FNe values show enrichment of Ne relative to ^{36}Ar. This failure of the CE model to fit the recharge parameters to the measured data is due to partitioning of the light and heavy noble gas compositions. One way this partitioning can occur is in the presence of a hydrocarbon phase in the subsurface. During groundwater mixing with a hydrocarbon phase, the solubility differences between hydrocarbons and groundwater preferentially partitions the heavy noble gases into the hydrocarbon phase; this process leaves the resulting groundwater depleted in the heavy and enriched in the light noble gases. This type of noble gas fluid phase partitioning can be modeled by simple Rayleigh fractionation of the noble gas components between the two fluid phases driven by the differences of solubility between phases (Ballentine et al., 2002).

We used a Rayleigh fractionation model of ASW (15 °C, 1,994-m elevation) encountering and losing noble gas components to a hydrocarbon phase using solubility coefficients for light oil (Kharaka and Specht, 1988) and water solubility coefficients (Crovetto et al., 1982) at an equilibration temperature of 30 °C. The fractionation trend (green dashed line in Fig. 7) begins with little change near the ASW value and progresses with greater partitioning and the loss of the heavier gases to the oil component. The calculations for Ne and Xe partitioning were made relative to the amount of Ar lost from the groundwater to the oil fraction (P-Ar 0.5 indicates 50% loss of the Ar component from the groundwater to the oil). The sample data remain offset from the Rayleigh fractionation modeled composition of oil/water interaction and ASW; this is likely explained as a mixture of ASW containing a partitioned oil/water component (mixing lines A and B in Fig. 7).

During the genesis of hydrocarbons from kerogen in a source rock, the compounds produced in the early stages of hydrocarbon formation interact with connate water trapped in the system to produce groundwaters that follow the trend of the oil/water

Table 7

Volatile organic carbon (VOC) compounds were detected at five sampled sites. Concentrations are in μg/L. Toluene was below the detection limit at all sites. Data from U.S. Geological Survey (2021).

	Well 228	Well 601	Well 602 (Chaco Well)				Well 64	Well 603		
Analyte	29–05–2019	27–08–2019	22–08–2017	28–05–2019	29–08–2019	04–06–2020	29–08–2019	29–05–2019	28–08–2019	04–06–2020
Benzene	0.072	0.044	0.044	0.049	0.054	0.044	1.08	< 0.026	0.019	< 0.026
Ethylbenzene	0.014	< 0.036	< 0.036	< 0.036	< 0.036	< 0.036	0.122	< 0.036	0.015	0.011
Napthalene	< 0.26	< 0.26	< 0.26	< 0.26	< 0.26	< 0.26	0.17	< 0.26	< 0.26	< 0.26
1,2,3,4 Tetramethylbenzene	< 0.1	< 0.01	–	< 0.01	< 0.01	< 0.01	0.05	< 0.01	< 0.01	< 0.01
o-Xylene	< 0.032	< 0.032	< 0.032	< 0.032	< 0.032	< 0.032	0.502	0.018	0.021	0.019
m-Xylene plus p-Xylene	< 0.08	0.05	< 0.08	< 0.08	< 0.08	< 0.08	0.05	0.04	0.04	0.03
2-Ethyltoluene	< 0.032	< 0.032	–	< 0.032	< 0.032	< 0.032	0.051	< 0.032	< 0.032	< 0.032
1,2,3 Trimethylbenzene	< 0.06	< 0.06	–	< 0.06	< 0.06	< 0.06	0.099	0.012	0.023	< 0.06
Isopropylbenzene	< 0.042	< 0.042	–	< 0.042	< 0.042	< 0.042	0.021	< 0.042	< 0.042	< 0.042
n-propylbenzene	< 0.036	< 0.036	< 0.036	< 0.036	< 0.036	< 0.036	0.01	< 0.036	< 0.036	< 0.036
1,2,4 Trimethylbenzene	< 0.032	0.019	< 0.032	< 0.032	< 0.032	< 0.032	< 0.032	0.024	0.039	0.021
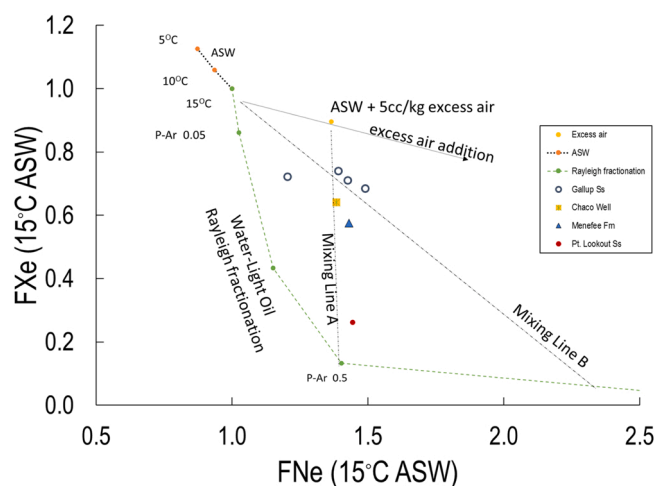
Fig. 7. Plot of FXe versus FNe. F values are defined as Csample/^{36}Ar of the sample normalized to CASW/^{36}Ar of fresh air saturated water (ASW) at 1,994-m elevation and 15 °C where C is the noble gas concentration. Note the propagated error is smaller than sample symbols. Green dots and the corresponding dashed line represent a water-light oil partition Rayleigh fractionation model done with ASW at 15 °C and at equilibrium with oil at 30 °C. The yellow dot with corresponding arrow labeled excess air addition represents ASW with 5cc/kg air addition. The burnt orange dots show ASW values at equilibrium with indicated temperatures. Mixing Line A represents mixing among ASW with excess air and groundwater slightly fractionated through interactions with hydrocarbons. Mixing Line B represents mixing between a much greater component of ASW with less excess air that is mixed with a much more partitioned component sourced from the shale. The point P-Ar 0.5 indicates a 50% loss of the Ar component from the groundwater to the oil.

partitioning from an air saturated source water. With ongoing hydrocarbon maturation, some amount of the connate groundwater present during the early stage of hydrocarbon formation is lost from the source rock (Bryne et al., 2020). These hydrocarbon waters presumably migrate to permeable units surrounding the source rock, forming a mix of ASW compositions and hydrocarbon water that is characteristic of mixing line B (Fig. 7). In noble gas samples taken from the Gallup Sandstone, Menefee Formation, and Point Lookout Sandstone aquifers, a large component of partitioned noble gas compositions sourced from the Mancos Shale seems to be mixed with an ASW component in the aquifers. The actual mixing could be ASW with some excess air and groundwater that is marginally fractionated with hydrocarbon groundwater (mixing line A in Fig. 7). Alternatively, the mixing could be through a much greater component of ASW with less excess air mixed with a much more partitioned component sourced from the hydrocarbon bearing shale (mixing line B in Fig. 7). The sample from the Point Lookout Sandstone (Well 603) is closest to the Rayleigh frationation modeled values for water/oil
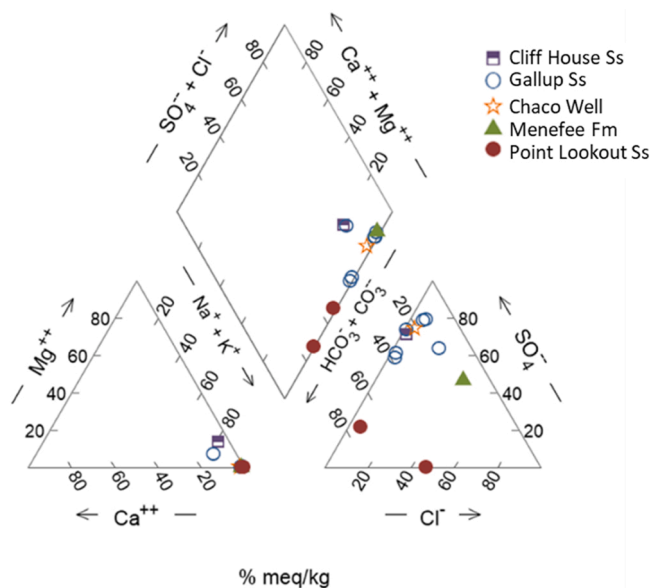
Fig. 8. Piper diagram showing major ion composition and geochemical water types of the aquifers sampled for this study. Abbreviations Ss and Fm stand for Sandstone and Formation, respectively.

partitioning and could in fact lie on the trend by adjusting the modeling temperature to 80°C instead of 30°C. As discussed below (Section 4.4), mixing with hydrocarbons could be facilitated by improperly cased boreholes in the region (Fig. 3 and 10).

4.2. Stable isotopes of oxygen and hydrogen

$\delta^{18}O$ and δ^2H results are shifted to the right of the local meteoric water line (LMWL; $\delta^2H=8\ \delta^{18}O + 12.5$, Vuataz and Goff, 1986) and may define a different meteoric water line or a past drier environment (Fig. 4). This result was repeated in Phillips et al. (1986) and Walvoord et al. (1999) who also found a right shift in the $\delta^{18}O$ and δ^2H isotopes in San Juan Basin groundwaters. Most Gallup Sandstone groundwaters sampled in our study have $\delta^{18}O$ values about 2‰ lighter than samples collected in the Cliff House Sandstone and Menefee Formation (Table 4). This could be driven by Gallup Sandstone recharge in the mountains south of the field area and lower elevation recharge in other formations. In Phillips et al. (1986), a relationship was found between ^{14}C and $\delta^{18}O$ whereby older groundwater was generally isotopically lighter than younger groundwater suggesting cooler climates during the Pleistocene. In the current study, older (>40,000 ybp) estimated ^{14}C ages are associated with heavier $\delta^{18}O$ and δ^2H values (Table 4). Although data are very limited, this could indicate some amount of climate warming between 40,000 and 20,000 ybp.

4.3. Geochemical evolution of groundwater

Groundwaters chemically evolve through time and over distances (Fisher ad Mullican, 1997); in this field area, they have had a long time to evolve (Section 3.3). Young groundwaters tend to have Ca-HCO₃ type water because carbonate minerals weather fastest imparting Ca^{2+} and HCO_3 ions. As calcite and dolomite saturation is reached, dissolution of silicate and gypsum minerals contribute SO_4^{2-} and Na^+ and Ca^{2+} and Mg^{2+} are exchanged for adsorbed Na^+. This geochemical evolution of groundwater produces Na-HCO₃ and Na-SO₄ type waters over long flow paths and time scales (Fisher and Mullican, 1997). All groundwater sites in this study are near calcite equilibrium and are supersaturated with dolomite and undersaturated with respect to gypsum (Table 6). A Piper diagram (Fig. 8) shows that the dominant cation in all groundwaters is sodium (Na^+); wells screened in the Point Lookout Sandstone are Na-HCO₃ type waters and the rest of the sampled sites have Na-SO₄ type water. This analysis suggests that groundwater in the Cliff House Sandstone is the least geochemically evolved and the Menefee Formation and Point Lookout Sandstone are the most geochemically evolved. In this section, we will show that Gallup Sandstone contains groundwater both relatively young at the southernmost sampling points (for the San Juan Basin) and highly geochemically evolved in the eastern and northern portion of the
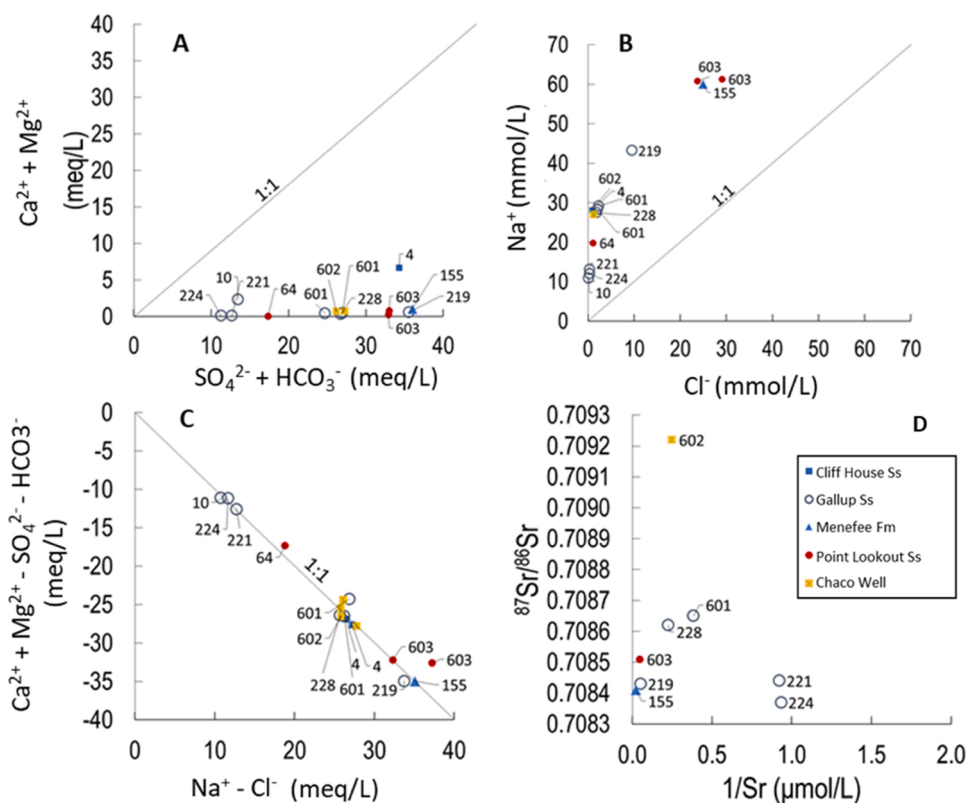
Fig. 9. Major ion and $^{87}Sr/^{86}Sr$ relationships used to decipher the geochemical evolution of groundwater. Samples show evidence of increasing geochemical evolution and silicate weathering along a flow path from the south to the north.

field area. Furthermore, there is evidence of mixing between aquifers.

If Ca^{2+}, Mg^{2+}, SO_4^{2-}, and HCO_3 are largely from the dissolution of calcite, dolomite, and gypsum, then these ions should be charge balanced, but they are not. In Fig. 9A, a ratio of 1:1 between Ca^{2+} + Mg^{2+} and SO_4^{2-} – HCO_3 would indicate mineral weathering of carbonates or gypsum. Instead, all waters plot below this line meaning that Na—the only other major cation—must balance the excess negative charge. All sites have molal ratios of Na^+ to Cl^- that exceed one (Fig. 9B). A ratio approximately equal to one would indicate halite dissolution while a ratio greater than one generally indicates Na^+ released from silicate weathering or cation exchange for Ca^{2+} and Mg^{2+} (Meybeck, 1987). Hence, in these samples, silicate weathering or cation exchange is likely contributing Na^+. Groundwater samples collected from the Menefee Formation and Point Lookout Sandstone are the only sites where Cl^- makes up a substantial portion of the anion balance. To test the importance of cation exchange, the relationships between Na^+ – Cl^- and Ca^{2+} + Mg^{2+} – SO_4^{2-} – HCO_3^- were examined (Fig. 9C). In this scenario, Na^+ – Cl^- (meq/L) represents the amount of Na^+ gained or lost from halite dissolution. Ca^{2+} + Mg^{2+} – SO_4^{2-} – HCO_3 represents the amount of Ca^{2+} and Mg^{2+} gained or lost relative to gypsum, calcite, and dolomite dissolution. If cation exchange is a dominant and controlling process, the relationship between these parameters will be linear with a slope of –1 (Fisher and Mullican, 1997). Fig. 9C shows that all groundwater samples plot along a straight line (R^2 =0.97) with a slope of –0.96. Hence, Ca^{2+} and Mg^{2+} ions have been exchanged for Na^+ through cation exchange. Gypsum dissolution also explains the relatively high SO_4 concentrations in many of the sampled groundwaters. In summary, groundwater in the field area is geochemically evolved with ions largely coming from cation exchange and gypsum dissolution. From this information, we infer that among wells in the Gallup Sandstone, wells from the southwest part of the field area (Wells, 10, 221, and 224) are the least geochemically evolved and wells 601, 602, and 228 to the north are more geochemically evolved. This is consistent with south to north groundwater flow as indicated by groundwater elevations (Table 1) and ^{14}C ages (Table 4). Well 219 also appears to be more geochemically evolved than other wells in the Gallup Sandstone though it is in the southern part of the field area; as discussed below (Section 4.4), this well is likely affected by mixing with adjacent aquifers.

In general, little variation in $^{87}Sr/^{86}Sr$ values was observed with the exception of Well 602, the Chaco Well, which had a higher $^{87}Sr/^{86}Sr$ value (Fig. 9D). It is presently unclear why the ratio was higher at this site, though higher $^{87}Sr/^{86}Sr$ ratios in groundwater are generally associated with greater weathering of potassium and rubidium rich minerals such K-feldspar and biotite (Cartwright et al., 2007).

4.4. Mixing between aquifers

Mixing between aquifers may be facilitated through improperly cased or plugged hydrocarbon wells in the region. The Chaco Well (Well 602) and Well 603 have 22 inactive hydrocarbon wells within 10 km and seven within 5 km (Fig. 3). Wells 155 and 219 have 24 hydrocarbon related boreholes wells within 1 km, all of which are drilled to the Menefee Formation, Morrison Formation, and to unknown depths (Fig. 10). Although these hydrocarbon wells are inactive, some could be conduits for vertical groundwater movement through relatively impermeable units such as the Mancos Shale (Kernodle, 1996; Lacombe et al., 1995).

A mixing line can be inferred from lower to higher concentrations of Na^+ versus Cl^- between Well 10 in the Gallup Sandstone and Wells 603 and 155 in the Point Lookout Sandstone and Menefee Formation, respectively (Fig. 9B). When examining HCO_3 and SO_4^{2-} concentrations against Na^+ (Figs. 11A and 11B), two divergent mixing pathways are seen, one towards Na-SO$_4$ type waters and the other towards Na-HCO$_3$ type waters. Again, the younger Well 10 (~23,000 ybp) is the more dilute end member and Wells 603 (>52,000 ybp) and 155 (~41,000 ybp) being the second and third end members with varying SO_4^{2-} and HCO_3 concentrations. These geochemical plots show that well 155, screened in the Menefee Formation and Well 603, screened in the Point Lookout Sandstone, represent distinct end members in the dataset. The low SO_4^- at Well 603 could be indicative of SO_4 reduction as this site which also had the highest NH_3 + NH_4 concentrations (Tables 2 and 5). Waters in the Gallup Sandstone and Cliff House Sandstone appear to be mixing with waters in the Menefee Formation instead of the Point Lookout Sandstone.

Cl^-/Br^- ratios are often used to help differentiate different water sources and infer sources of produced water (Davis et al., 1998; Ziemkiewicz, Thomas, 2015). For example, groundwaters with Cl^-/Br^- molar ratios > 2500 are likely mixing with brine (Davis et al., 1998) while produced waters may carry excess Br^- potentially lowering the Cl^-/Br^- ratio (Tasker et al., 2020; Ziemkiewicz, Thomas, 2015). In this study, Cl^-/Br^- molar ratios varied between 229.8 and 5,409.1 with the lowest and highest values coming from Well 4 (Cliff House Sandstone) and Well 603 (Point Lookout Sandstone), respectively. In Fig. 11 C, Cl^-/Br^- ratios are highest for Wells 155 and 603 screened in the Menefee Formation and Point Lookout Sandstone, respectively. As evidenced by the noble gas results (Section 3.1), water in Well 603 may be mixing with shale connate waters expelled during hydrocarbon formation. Water from Well 155 may also be mixing with a brine water.

Vertical mixing between aquifers is known to occur in the San Juan Basin, generally with low rates through shale beds and higher leakage rates in localized areas associated with faults and fractures (Stone et al., 1983); furthermore, vertical gradients were found in this study which could help induce mixing (Table 1). Mixing between aquifers is evident between geochemical end members represented by the youngest (Section 3.2) and most dilute Gallup Sandstone sample collected (Well 10) and the much more saline Well 155 (Menefee Formation) and Well 603 (Point Lookout Sandstone); this also could include mixing between an unsampled aquifer deeper in the region. Well 219, screened in the Gallup Sandstone, is geochemically similar to Well 155 in all geochemical figures including the carbon isotopes (Fig. 5), $\delta^{18}O$ and δ^2H (Fig. 4), strontium isotopes (Fig. 9D), and major ion chemistry (Figs. 6, 8, 9, and 11). The Chaco Well appears to be intermediate between the Gallup Sandstone and the Menefee Formation and Cliff House Sandstone end members. The direction of mixing in the basin is likely from deeper to shallower depths as indicated by the groundwater level measurements (Table 1); it is possible that deeper unsampled groundwaters moving vertically through formations or through improperly cased boreholes are strongly influencing groundwater chemistry. This may be the case in Wells 219 (Gallup Sandstone aquifer) and 155
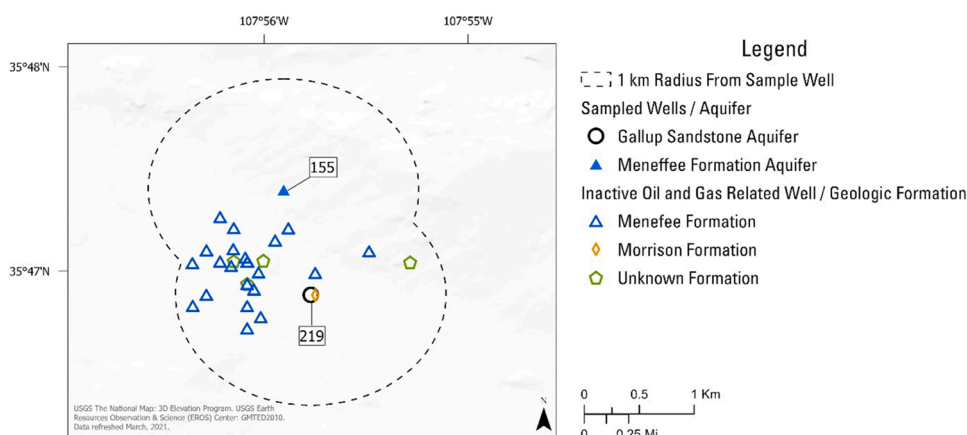
Fig. 10. All known hydrocarbon related boreholes within a 1-km radius of Wells 155 and 219. Oil and gas well locations and information is available through the State of New Mexico Oil Conservation Division: https://www.emnrd.nm.gov/ocd/#gsc.tab= 0.
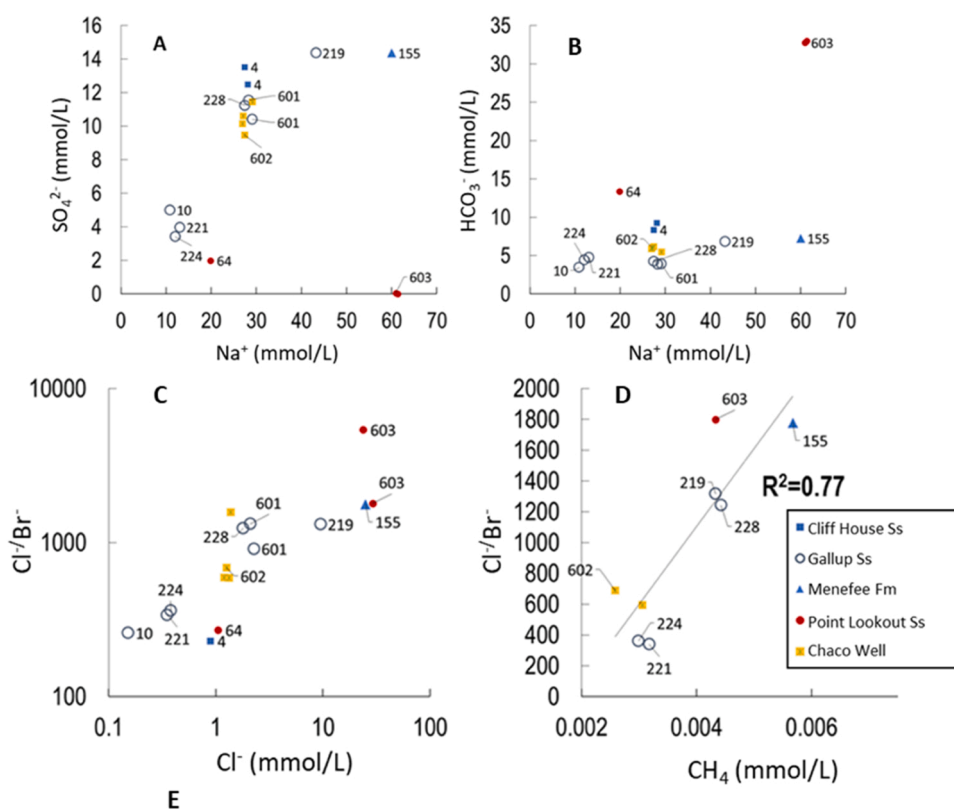
Fig. 11. Plots A and B: Sulfate versus Na^+ and HCO_3 versus Na+ in sampled groundwaters. These plots demonstrate that well 603, 155, and 10 represent three end members in the hydrochemical dataset. Plots C and D: molar ratios of Cl^-/Br^- versus Cl^- and methane (CH_4) concentrations.

(Menefee Formation) where the many nearby inactive hydrocarbon boreholes (Fig. 10) could have facilitated vertical mixing and groundwater chemistry homogenization.

Implications of this research is that while groundwater movement is slow, vertical mixing between aquifers is likely occurring despite the less permeable Mancos Shale that separates the Gallup Sandstone and the surrounding aquifers. This mixing could be augmented through the many boreholes drilled throughout the field area (Figs. 3 and 10). Hence, contaminants from hydrocarbon extraction activities in the San Juan Basin may travel between aquifers and could be affecting water quality in the Gallup Sandstone aquifer.

4.5. Detections of hydrocarbon related compounds and the possibility of contamination from hydrocarbon extraction activities

Though naturally occurring, BTEX and other VOC detections may be explained by leakage from improperly cased or failed casings of nearby oil and gas wells (Figs. 3 and 10). For example, Chaco Well is 5 km directly north from an inactive hydrocarbon borehole drilled into the Gallup Sandstone aquifer. Given the age of the hydrocarbon well (1956), groundwater flow directions (south to north), and the conductivity of the Gallup Sandstone aquifer (111 m/y; Kernodle, 1996), it is possible that contaminants could have migrated vertically through the borehole and then horizontally ~7 km towards the Chaco Well.

The three Gallup Sandstone aquifer wells with VOC detections were located on the north and east side of the study area downgradient of Gallup Sandstone wells with no VOC detections. The downgradient water may represent older more evolved groundwater that has had more interaction with hydrocarbon deposits or leakage through boreholes from adjacent stratigraphic units with hydrocarbon deposits.

In addition to evidence from noble gas analyses which suggests influence from connate water expelled from shale during hydrocarbon formation (Section 4.1), Well 603 had highly elevated barium (Ba; 60–73 μmol/L; Table 5), relatively high Cl$^-$ (28.21–29.05 mmo/L), and bromide (0.0125–0.0161 mmol/L). These elements are commonly present in high concentrations in oil field brines and shale waters (Barbot et al., 2013; Hudak and Wachal, 2001; Ziemkiewicz, Thomas, 2015). Notably, the Cl$^-$/Br$^-$ molar ratio changed from 5409 to 1799 between 1987 and 2019 at Well 603 and in 2019, the well contained trace VOC detections. The drop in Cl$^-$/Br$^-$ is consistent with a new source of Br$^-$ rich brine water though TDS did not change appreciably. CH_4 concentrations were also significantly correlated to the Cl$^-$/Br$^-$ ratio (Fig. 11D), a finding that could implicate a similar source for high Cl$^-$/Br$^-$ and CH_4. However, both CH_4 and high Cl$^-$/Br$^-$ ratios often have natural origins and could indicate mixing with a CH_4 containing shale water (Davis et al., 1998; Li et al., 2016; Ziemkiewicz, Thomas, 2015). Furthermore, the Point Lookout Sandstone aquifer waters had high CH_4 and low SO_4^- potentially indicating in situ methanogenesis. Further work could measure stable H and C isotopes of CH_4 to help distinguish methane sources (Bernard et al., 1976).

This study did not examine synthetic chemicals that could confirm direct effect from hydrocarbon extraction activities. Further work to determine whether hydrocarbon extraction activities such as HF are affecting drinking water resources in the San Juan Basin and at CCNHP could sample for synthetic organic compounds such as diethylene glycol and per- and polyfluoroalkyl substances (PFAS). The U.S. Environmental Protection Agency reported diethylene glycol in groundwater near an extensive shale gas operation in Pavillion, Wyoming (Di Giulio et al., 2011). PFAS are extremely recalcitrant compounds—often termed forever chemicals—that are used in large quantities during hydrocarbon extraction (Glüge et al., 2020; Meng et al., 2021). In a recent study of groundwater and soils near oil fields, substantially higher concentrations of PFAS were observed downgradient of oil fields compared to upgradient (Meng et al., 2021). Further work pairing these synthetic compounds with noble gas, major ion, VOC, and isotope analyses could help determine the sources of VOCs found in groundwater at CCNHP and the greater San Juan Basin. Despite the extensive amount of hydrocarbon extraction taking place, geochemical groundwater data in the region is sparse; further work studying the effect of hydrocarbon extraction on water quality and quantity in the San Juan Basin could fill some of these knowledge gaps.

5. Conclusions

Despite the large number of hydrocarbon extraction wells in the San Juan Basin, very little is known of the groundwater chemistry, flow directions, or the potential impact oil and gas related wells could have on drinking water sources. This work shows that mixing between aquifers, even through the relatively impermeable Mancos Shale (Kernodle, 1996), is possible and may be facilitated through the numerous inactive oil and gas related boreholes in the region. Given groundwater conductivity through the Gallup Sandstone aquifer (111 m/y; Kernodle, 1996), it is possible that contaminants from nearby oil and gas wells targeting and not targeting the Gallup Sandstone could nevertheless migrate vertically and then, over the course of years to decades, move to the main drinking water source at CCNHP (Well 602, Chaco Well). Furthermore, the lack of modern water in the sampled aquifers indicates that any water extraction will not be replaced by modern recharge.

Several lines of evidence suggest groundwater contamination from nearby oil and gas extraction activity is possible or has occurred. First, noble gas results imply mixing with waters that have interacted with hydrocarbons (Section 4.1); second, the presence of VOCs—including BTEX compounds—also indicates interaction with hydrocarbon fluids; lastly, mixing between aquifers is supported by major ion and isotopic geochemical analyses. This study establishes baseline geochemistry and groundwater flow direction (from south to north) for seldom sampled aquifers in the San Juan Basin that can serve to compare with future studies.

Whether the mixing and presence of VOC compounds is naturally occurring or is facilitated through oil and gas related boreholes will require further investigation. Further work could endeavor to analyze groundwater for synthetic chemicals used during HF (Mumford et al., 2018) especially at the Chaco Well (Gallup Sandstone) and Well 603 (Point Lookout Sandstone). Further study could also benefit from sampling produced and flowback water from active oil and gas wells to help determine the organic compounds and geochemistry that could help trace produced waters. Additional work could also seek to measure the stable isotopes of CH_4 to help determine the sources of CH_4 in the aquifer (McIntosh et al., 2018).

CRediT authorship contribution statement

Benjamin S. Linhoff: Project conceptualization, methodology, formal analysis, investigation, resources, writing original draft, writing review and editing, visualization of figures, supervision of project staff, project administration, and funding acquisition, **Kimberly R. Beisner:** Project methodology, formal analysis, writing original draft, editing final draft, and validation of data, **Andrew**

G. Hunt: Formal analysis, writing original draft, **Zachary M. Shephard:** Writing original draft, writing review and editing, visualization.

Declaration of Competing Interest

Data Availability

All data used are available through the U.S. Geological Survey National Water Information System Database: https://waterdata.usgs.gov/nwis.

Acknowledgments

Appendix A. Supporting information

Supplementary data associated with this article can be found in the online version at doi:10.1016/j.ejrh.2023.101430.

References

Aeschbach-Hertig, W., Peeters, F., Beyerle, U., Kipfer, R., 1999. Interpretation of dissolved atmospheric noble gases in natural waters. Water Resour. Res. v. 35 (9), 2779–2792.

Ballentine, C.J., Burgess, R., Marty, B., 2002. Tracing Fluid Origin, Transport and Interaction in the Crust. In: Porcelli, D., Ballentine, C.J., Wieler, R. (Eds.), Noble Gases in Geochemistry and Cosmochemistry. Mineralogical Society of America, Washington D.C., pp. 481–538

Barbot, E., Vidic, N.S., Gregory, K.B., Vidic, R.D., 2013. Spatial and temporal correlation of water quality parameters of produced waters from Devonian-age shale following hydraulic fracturing. Environ. Sci. Technol. v. 47 (6), 2562–2569.

Bernard, B.B., Brooks, J.M., Sackett, W.M., 1976. Natural gas seepage in the Gulf of Mexico. Earth Planet. Sci. Lett. 31 (1), 48–54.

Brister, B.S., and G.K. Hoffman. 2002. Fundamental geology of San Juan Basin energy resources. Pages 21–25 in B.S. Brister and L.G. Price, editors. New Mexico's energy, present and future: policy, production, economics, and the environment. Decision Makers Field Conference 2002. New Mexico Bureau of Geology and Mineral Resources, Socorro, New Mexico. http://geoinfo.nmt.edu/publications/guides/decisionmakers/2002/ (Accessed 27 January 2023).

Bryan, S., 2023, Court: US needs to consider effects of drilling near Chaco, Associated Press, https://apnews.com/article/politics-united-states-government-bureau-of-land-management-climate-and-environment-business-f4aaa217511adc62cac313d0ea5bd0f5 (Accessed 4 February 2023).

Bullen, T.D., Krabbenhoft, D., Kendall, C., 1996. Kinetic and mineralogic controls on the evolution of groundwater chemistry and ^{87}Sr/^{86}Sr in a sandy silicate aquifer, v. 60. Geochimica et Cosmochimica Acta, northern Wisconsin, USA, pp. 1807–1821. https://doi.org/10.1016/0016-7037(96)00052-X.

Byrne, D.J., Barry, P.H., Lawson, M., Ballentine, C.J., 2020. The use of noble gas isotopes to constrain subsurface fluidflow and hydrocarbon migration in the East Texas Basin. GCA 268, 186–208.

Cartwright, I., Weaver, T., Petrides, B., 2007. Controls on ^{87}Sr/^{86}Sr ratios of groundwater in silicate-dominated aquifers, v. 246. Chemical Geology, SE Murray Basin, Australia, pp. 107–123.

Cartwright, I., Currell, M.J., Cendón, D.I., Meredith, K.T., 2020. A review of the use of radiocarbon to estimate groundwater residence times in semi-arid and arid areas. J. Hydrol. 580, 124247.

Clark, C.E., Horner, R.M., Harto, C.B., 2013. Life cycle water consumption for shale gas and conventional natural gas. Environ. Sci. Technol. v. 47 (20), 11829–11836.

Connor, B.F., Rose, D.L., Noriega, M.C., Murtagh, L.K., and Abney, S.R., 1998, Methods of Analysis by the U.S. Geological Survey National Water Quality Laboratory — Determination of 86 Volatile Organic Compounds in Water by Gas Chromatography/Mass Spectrometry, Including Detections Less Than Reporting Limits, U.S. Geological Survey Open-File Report 97–829, 78p, https://nwql.usgs.gov/pubs/OFR/OFR-97–829.pdf.

Cozzarelli, I.M., Skalak, K.J., Kent, D.B., Engle, M.A., Benthem, A., Mumford, A.C., Haase, K., Farag, A., Harper, D., Nagel, S.C., Iwanowicz, L.R., 2017. Environmental signatures and effects of an oil and gas wastewater spill in the Williston Basin, North Dakota. Sci. Total Environ. 579, 1781–1793.

Cozzarelli, I.M., Kent, D.B., Briggs, M., Engle, M.A., Benthem, A., Skalak, K.J., Mumford, A.C., Jaeschke, J., Farag, A., Lane Jr, J.W., Akob, D.M., 2021. Geochemical and geophysical indicators of oil and gas wastewater can trace potential exposure pathways following releases to surface waters. Sci. Total Environ. 755, 142909.

Crovetto, R., Fernández-Prini, R., Japas, M.L., 1982. Solubilities of inert gases and methane in H2O and in D2O in the temperature range of 300 to 600 K. The. J. Chem. Phys. 76 (2), 1077–1086.

Dam, W.L., 1995. Geochemistry of ground water in the, Dakota, and Morrison aquifers, San Juan Basin, 94. Water-Resources Investigations Report,, New Mexico, p. 4253.

Davis, S.N., Whittemore, D.O., Fabryka-Martin, J., 1998. Uses of chloride/bromide ratios in studies of potable water. Ground Water v. 36 (2), 338–350.

Di Giulio D.C., Wilkin R.T., Miller C., Oberley G., 2011, Investigation of Ground Water Contamination near Pavillion, Wyoming. U.S. Environmental Protection Agency Report 2011 http://www.epa.gov/region8/superfund/wy/pavillion/.

Engler, T., W., Kelley, S., Cather, M, 2015, Reasonable foreseeable development (RFD) for northern New Mexico: New Mexico Bureau of Geology and Mineral Resources Open-file Report 567.

Federal Geographic Data Committee [prepared for the Federal Geographic Data Committee by the U.S. Geological Survey] , 2006, FGDC Digital Cartographic Standard for Geologic Map Symbolization: Reston, Va., Federal Geographic Data Committee Document Number FGDC-STD-013–2006, 290 p., 2 plates.

Fisher, S.R., Mullican, W.F.I., 1997. Hydrochemical evolution of sodium-sulfate and sodium-chloride groundwater beneath the northern Chihuahuan Desert, v. 5. Hydrogeology Journal,, Trans-Pecos, Texas, USA.

Fishman, M.J., and Friedman, L.C., 1989, Methods for determination of inorganic substances in water and fluvial sediments: U.S. Geological Survey Techniques of Water-Resources Investigations, book 5, chap. A1, 545 p., https://doi.org/10.3133/twri05A1.

Fishman, M.J., ed., 1993, Methods of analysis by the U.S. Geological Survey National Water Quality Laboratory— Determination of inorganic and organic constituents in water and fluvial sediments: U.S. Geological Survey Open File Report 93–125, 217 p., at https://doi.org/10.3133/ofr93125.

Gallegos, T.J., and Varela, B.A., 2015, Data Regarding Hydraulic Fracturing Distributions and Treatment Fluids, Additives, Proppants, and Water Volumes Applied to Wells Drilled in the United States from 1947 through 2010: US Geological Survey Data Series 868, p. 11.

Glüge, J., Scheringer, M., Cousins, I.T., Dewitt, J.C., Goldenman, G., Herzke, D., Lohmann, R., Ng, C.A., Trier, X., and Wang, Z., 2020, An overview of the uses of per- and polyfluoroalkyl substances (PFAS): 2345–2373 p.

Gordalla, B.C., Ewers, U., Frimmel, F.H., 2013. Hydraulic fracturing: a toxicological threat for groundwater and drinking-water? Environ. Earth Sci. 70 (2013), 3875–3893. https://doi.org/10.1007/s12665-013-2672-9.

Han, L.F., Plummer, L.N., 2016. A review of single-sample-based models and other approaches for radiocarbon dating of dissolved inorganic carbon in groundwater. Earth-Sci. Rev. 152, 119–142.

Han, L.F., Plummer, L.N., Aggarwal, P., 2012. A graphical method to evaluate predominant geochemical processes occurring in groundwater systems for radiocarbon dating. Chem. Geol. 318–319, 88–112. https://doi.org/10.1016/j.chemgeo.2012.05.004.

Han, L.-F., Plummer, L.N., 2013. Revision of Fontes & Garnier's model for the initial ^{14}C content of dissolved inorganic carbon used in groundwater dating. Chem. Geol. v. 351, 105–114. https://doi.org/10.1016/j.chemgeo.2013.05.011.

Heaton, T.H.E., Vogel, J.C., 1981. "Excess air" in groundwater. J. Hydrol. v. 50, 21–216.

Hudak, P.F., Wachal, D.J., 2001. Effects of brine injection wells, dry holes, and plugged oil/gas wells on chloride, bromide, and barium concentrations in the Gulf Coast Aquifer, southeast Texas, USA. Environ. Int. v. 26 (7–8), 497–503.

Hunt, A.G., 2015, Noble Gas Laboratory's standard operating procedures for the measurement of dissolved gas in water samples: U.S. Geological Survey Techniques and Methods, book 5, chap. A11, 22 p., https://doi.org/10.3133/tm5A11.

Jurgens, B.C., Böhlke, J.K., Haase, K., Busenberg, E., Hunt, A.G. and Hansen, J.A., 2020. DGMETA (version 1)—Dissolved gas modeling and environmental tracer analysis computer program (No. 4-F5). US Geological Survey.

Karolyte, R., Barry, P.H., Hunt, A.G., Kulongoski, J.T., Tyne, R.L., Davis, T.A., Wright, M.T., McMahon, P.B., Ballentine, C.J., 2021. Noble gas signatures constrain oil-field water as the carrier phase of hydrocarbons occurring in shallow aquifers in the San Joaquin Basin, USA. Chem. Geol. 584 https://doi.org/10.1016/j.chemgeo.2021.120491.

Kelley, S., Engler, T., Cather, M., Pokorny, C., Yang, C., Mamer, E., Hoffman, G., Wilch, J., Johnson, P., Zeigler, K., 2014. Hydrologic Assessment of Oil and Gas Resource Development of the Mancos Shale in the San Juan Basin. N. Mex. N. Mex. Bur. Geol. Miner. Resour. Open-file Rep. 566.

Kernodle, J.M., 1996, Hydrogeology and steady-state simulation of ground-water flow in the San Juan Basin, New Mexico, Colorado, Arizona, And Utah: U. S. Geological Survey Water-Resources Investigation Report 95–4187, https://doi.org/10.3133/wri954187.

Kharaka, Y.K., Specht, D.J., 1988. The solubility of noble gases in crude oil at 25–100C. Appl. Geochem. 3 (2), 137–144.

Lacombe, S., Sudicky, E.A., Frape, S.K., Unger, A.J.A., 1995. Influence of leaky boreholes on cross-formational groundwater flow and contaminant transport. Water Resour. Res. 31 (8), 1871–1882. https://doi.org/10.1029/95WR00661.

Lekson, S.H., 1984. Great Pueblo architecture of Chaco Canyon, Joan Mathien and Randall H. Mcguire. Southern Illinois Univ. Press, Carbondale, pp. 243–269.

Li, J., Li, X., Wang, X., Li, Y., Wu, K., Shi, J., Yang, L., Feng, D., Zhang, T., Yu, P., 2016. Water distribution characteristic and effect on methane adsorption capacity in shale clay. Int. J. Coal Geol. 159, 135–154.

Lindsey, B.D., Jurgens, B.C., and Belitz, K., 2019, Tritium as an indicator of modern, mixed, and premodern groundwater age: U.S. Geological Survey Scientific Investigations Report 2019–5090, 18 p., https://doi.org/10.3133/sir20195090.

Linhoff, B., 2022. Deciphering natural and anthropogenic nitrate and recharge sources in arid region groundwater. Sci. Total Environ., 157345 https://doi.org/10.1016/j.scitotenv.2022.157345.

McIntosh, J.C., Ferguson, G., 2019. Conventional oil—the forgotten part of the water-Energy nexus. Groundwater 57 (5), 669–677. https://doi.org/10.1111/gwat.12917.

McIntosh, J.C., Hendry, M.J., Ballentine, C., Haszeldine, R.S., Mayer, B., Etiope, G., Elsner, M., Darrah, T.H., Prinzhofer, A., Osborn, S., Stalker, L., 2018. A critical review of state-of-the-art and emerging approaches to identify fracking-derived gases and associated contaminants in aquifers. Environ. Sci. Technol. 53 (3), 1063–1077.

McMahon, P.B., Barlow, J.R.B., Engle, M.A., Belitz, K., Ging, P.B., Hunt, A.G., Jurgens, B.C., Kharaka, Y.K., Tollett, R.W., Kresse, T.M., 2017. Methane and benzene in drinking-water wells overlying the Eagle Ford, Fayetteville, and Haynesville Shale hydrocarbon production areas. Environ. Sci. Technol. 51, 6727–6734.

Meng, Q., Ashby, S., 2014. Distance: a critical aspect for environmental impact assessment of hydraulic fracking. Extr. Ind. Soc. 1 (2014), 124–126.

Meng, Y., Yao, Y., Chen, H., Li, Q., Sun, H., 2021. Legacy and emerging per- and polyfluoroalkyl substances (PFASs) in Dagang Oilfield: Multimedia distribution and contributions of unknown precursors. J. Hazard. Mater. v. 412 (no. January).

Meybeck, M., 1987. Global chemical weathering of surficial rocks estimated from river dissolved loads. Am. J. Sci. v. 287, 401–428.

Moe, R., 2017, The Treasures of Chaco Canyon Are Threatened by Drilling: The New York Times. https://www.nytimes.com/2017/12/01/opinion/chaco-canyon-new-mexicodrilling.htm.

Mumford, A.C., Akob, D.M., Klinges, J.G., Cozzarelli, I.M., 2018. Common hydraulic fracturing fluid additives alter the structure and function of anaerobic microbial communities. Appl. Environ. Microbiol 84, e02729–17. https://doi.org/10.1128/AEM.02729-17.

National Park Service (NPS), 2015, Foundation Document Chaco Culture National Historical Park New Mexico, https://www.nps.gov/CCNHP/getinvolved/upload/CCNHP_FD_PRINT.pdf.

Njobuenwu, D.O., Amadi, S.A., Ukpaka, P.C., 2005. Dissolution rate of BTEX contaminants in water. Can. J. Chem. Eng. 83, 985–989.

Parkhurst, D.L., and Charlton, S.R., 2008, NetpathXL—An Excel® interface to the program NETPATH: U.S. Geological Survey Techniques and Methods 6–A26, 11 p.

Patton, C.J., and Kryskalla, J.R., 2011, Colorimetric determination of nitrate plus nitrite in water by enzymatic reduction, automated discrete analyzer methods: U.S. Geological Survey Techniques and Methods, book 5, chap. B8, 34 p., https://doi.org/10.3133/tm5B8.

Perra, C., A., 2021, Investigating cross formational flow of fluids through oil and gas wells in Alberta and Saskatchewan, Canada, Thesis, Department of Civil, Geological and Environmental Engineering, University of Saskatchewan, Saskatoon, Canada, 157 pp.

Phillips, F.M., Peeters, L., Tansey, M., 1986. Paleoclimatic inferences from an isotopic investigation of groundwater in the central San Juan Basin, no. 26. Quaternary Research, New Mexico, pp. 179–193.

Ran, J., Qiu, H., Sun, S., Tian, L., 2018. Short-term effects of ambient benzene and TEX (toluene, ethylbenzene, and xylene combined) on cardiorespiratory mortality in Hong Kong. Environ. Int. 117, 91–98.

Révész, K., and Coplen, T.B., 2008, Determination of the δ2H/1H, of water—RSIL lab code 1574: U.S. Geological Survey Techniques and Methods, book 10, chap. C1, 27 p., at https://doi.org/10.3133/tm10C1.

Rose, D.L., Sandstrom, M.W., and Murtagh, L.K., 2016, Determination of heat purgeable and ambient purgeable volatile organic compounds in water by gas chromatography/mass spectrometry: U.S. Geological Survey Techniques and Methods, book 5, chap. B12, 61 p., https://doi.org/10.3133/tm5B12.

Solder, J.E., Beisner, K.R., Anderson, J., Bills, D.J., 2020. Rethinking groundwater flow on the South Rim of the Grand Canyon, USA: characterizing recharge sources and flow paths with environmental tracers. Hydrogeol. J. 28 (5), 1593–1613. https://doi.org/10.1007/s10040-020-02193-z.

Spycher, B.D., Lupatsch, J.E., Huss, A., Rischewski, J., Schindera, C., Spoerri, A., Vermeulen, R., Kuehni, C.E., Swiss Paediatric Oncology Group and Swiss National Cohort Study Group, 2017. Parental occupational exposure to benzene and the risk of childhood cancer: a census-based cohort study. Environ. Int. 108, 84–91.

Stone, W.J., Lyford, F.P., Frenzel, P.F., Mizell, N.H., and Padgett, E.T., 1983, Hydrogeology and water resources of San Juan Basin, New Mexico: Socorro, New Mexico Bureau of Mines and Mineral Resources Hydrologic Report 6, 70p.

Stringfellow, W.T., Domen, J.K., Camarillo, M.K., Sandelin, W.L., Borglin, S., 2014. Physical, chemical, and biological characteristics of compounds used in hydraulic fracturing. J. Hazard. Mater. 275, 37–54. https://doi.org/10.1016/j.jhazmat.2014.04.040.

Stute, M., Sonntag, C., 1992. Paleotemperatures derived from noble gases dissolved in groundwater in relation to soil temperature. In: Staff, I.A.E.A. (Ed.), Isotopes of Noble Gases as Tracers in Environmental Studies. IAEA, Vienna, pp. 111–122.

Tasker, T.L., Warner, N.R., Burgos, W.D., 2020. Geochemical and isotope analysis of produced water from the Utica/Point Pleasant Shale, Appalachian Basin. Environ. Sci.: Process. Impacts 22 (5), 1224–1232. https://doi.org/10.1039/d0em00066c.

Travis, R.E., Bell, M.T., Linhoff, B.S. and Beisner, K.R., 2021. Utilizing multiple hydrogeologic and anthropogenic indicators to understand zones of groundwater contribution to water-supply wells near Kirtland Air Force Base Bulk Fuels Facility in southeast Albuquerque, New Mexico (No. 2021–5076). US Geological Survey, https://doi.org/10.3133/sir20215076.

U.S. Energy Information Administration, 2015. Annual Energy Outlook 2015. . Integr. Int. Energy Anal. 1, 1–244 https://doi.org/DOE/EIA-0383(2013).

U.S. Geological Survey. (2021). USGS water data for the Nation: U.S. Geological Survey National Water Information System database, accessed [2/15/2021], at https://doi.org/10.5066/F7P55KJN.

Vuataz, F.D., Goff, F., 1986. Isotope geochemistry of thermal and nonthermal waters in the Valles Caldera, Jemez Mountains, northern New Mexico. J. Geophys. Res.: Solid Earth 91 (B2), 1835–1853.

Walvoord, M.A., Pegram, P., Phillips, F.M., Person, M., Kicft, T.L., Fredrickson, J.K., Mckinley, J.P., Swenson, J.B., 1999. Groundwater flow and geochemistry in the southeastern San Juan Basin: implications for microbial transport and activity. Water Resour. v. 35 (5), 1409–1424.

Weiss, R.F., 1968. Piggyback sampler for dissolved gas studies on sealed water samples. Deep-Sea Res. v. 15, 695–699.

Wen, T., Liu, M., Woda, J., Zheng, G., Brantley, S.L., 2021. Detecting anomalous methane in groundwater within hydrocarbon production areas across the United States. Water Res. 200, 117236 https://doi.org/10.1016/j.watres.2021.117236.

Ziemkiewicz, P.F., Thomas, He, Y., 2015. Evolution of water chemistry during Marcellus Shale gas development: a case study in West Virginia. Chemosphere v. 134, 224–231.